

БИОРАСПРЕДЕЛЕНИЕ ВЫСОКОПОРИСТЫХ ЧАСТИЦ КАРБОНАТА КАЛЬЦИЯ С ПОЛИМЕРНЫМИ ОБОЛОЧКАМИ В ЖИВОТНЫХ- ОПУХОЛЕНОСИТЕЛЯХ

Т.Н. Паллаева¹, О.Ю. Грязнова²,
Д.А. Еуров³, Д.А Курдюков³,
В.К. Попова⁴, Е.В. Дмитриенко⁴,
Д.Б. Трушина^{1,5}

¹ ФНИЦ «Кристаллография и фотоника»
РАН, Москва

² ИБХ РАН, Москва

³ ФТИ им. А.Ф. Иоффе, Санкт-Петербург

⁴ Институт химической биологии и
фундаментальной медицины СО РАН,
Новосибирск,

⁵ Первый МГМУ им. И.М. Сеченова,
Москва

Trushina.d@mail.ru



CaCO_3 applications

Metallurgy and building

Manufacture of paints, paper, rubber, plastics, glass...

Cosmetics, personal hygiene products

Food industry

Water decontamination

Medicine

White color

Anti-caking property

Mechanical properties

Physical stability

Low cost

Biocompatibility

Low toxicity

Mild decomposition conditions

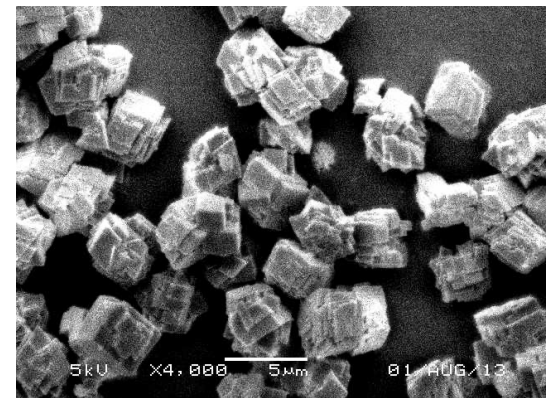
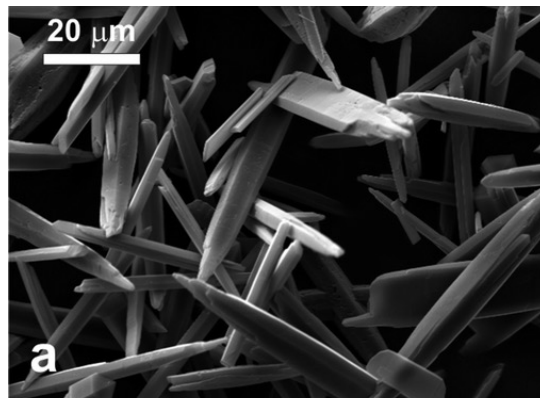
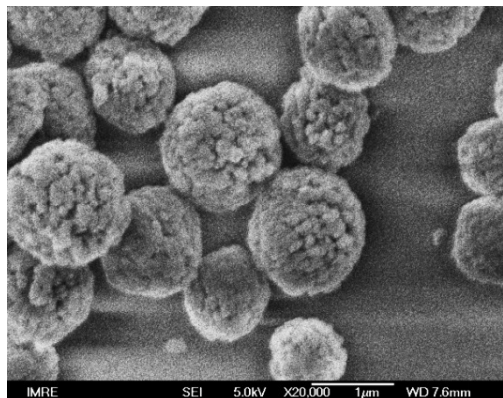
Biodegradability

Good absorption capacity

Ability to control particle parameters



CaCO_3 Polymorphism



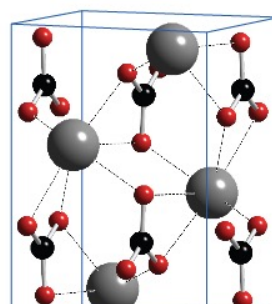
Metastable

Stable

Porous structure
Developed surface
↓
Efficient loading of active
molecules

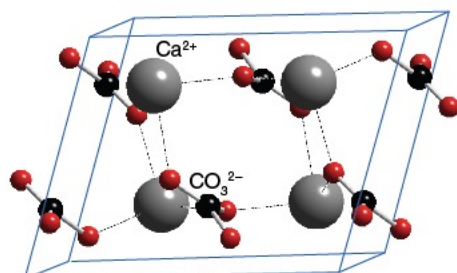
Vaterite

Hexagonal crystal system



Aragonite

Orthorhombic
crystal system

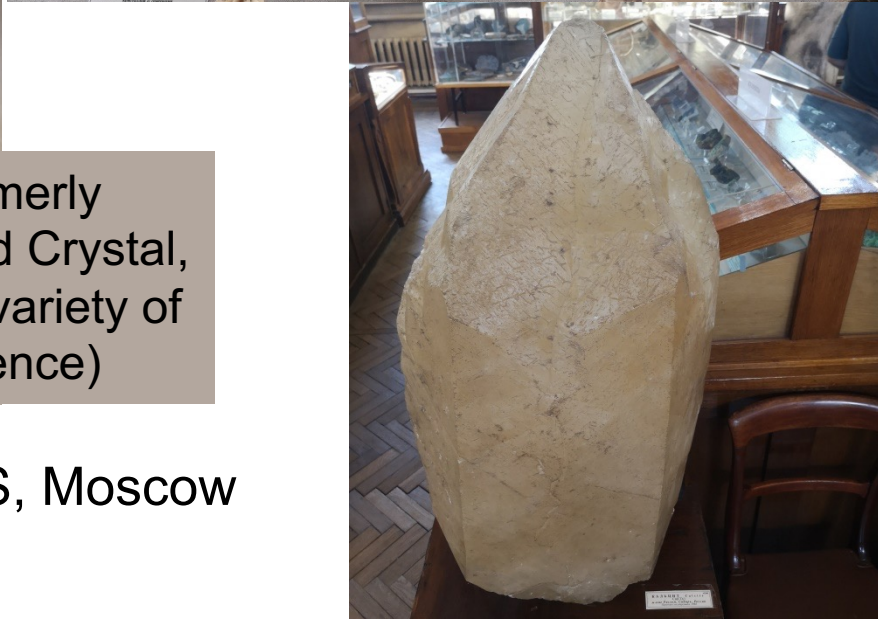


Calcite

Trigonal crystal system

CaCO_3 particles: 3 polymorphs

Calcite



Iceland spar, formerly known as Iceland Crystal, is a transparent variety of calcite (birefringence)

Fersman Mineralogical Museum RAS, Moscow

CaCO_3 particles: 3 polymorphs Aragonite



АРАГОНИТ CaCO_3 ARAGONITE
Кристаллиты дорастающие из отдельных кристаллов.
Хайдаркан, Киргизия.
Степанов В.И. (коллекция) (1984)

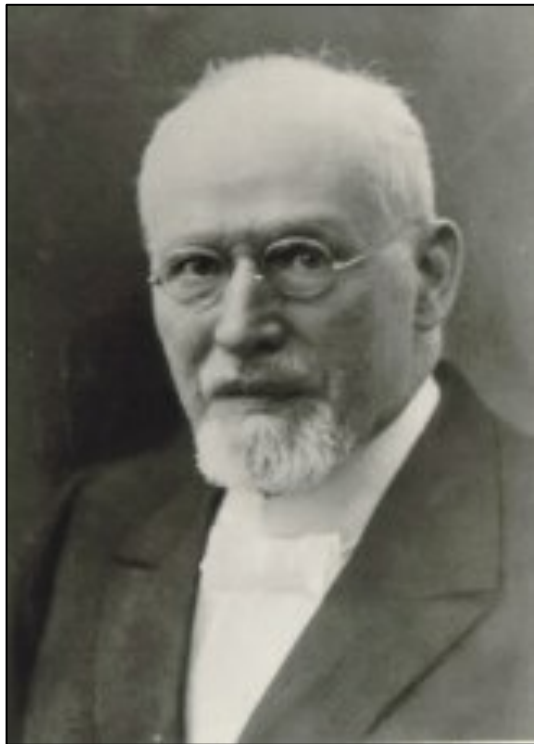
2062 №
АРАГОНИТ CaCO_3 ARAGONITE
Ажурный хрустящий каркас из кристаллитиков.
пещера Гиссаса, Хайдаркан, Киргизия.
Степанов В.И. (коллекция) 1969



Fersman Mineralogical Museum RAS, Moscow

CaCO_3 particles: 3 polymorphs

Vaterite (1903) is less stable form of CaCO_3



Heinrich Vater

was a pioneer in the forest soil science, land evaluation, forest fertilization

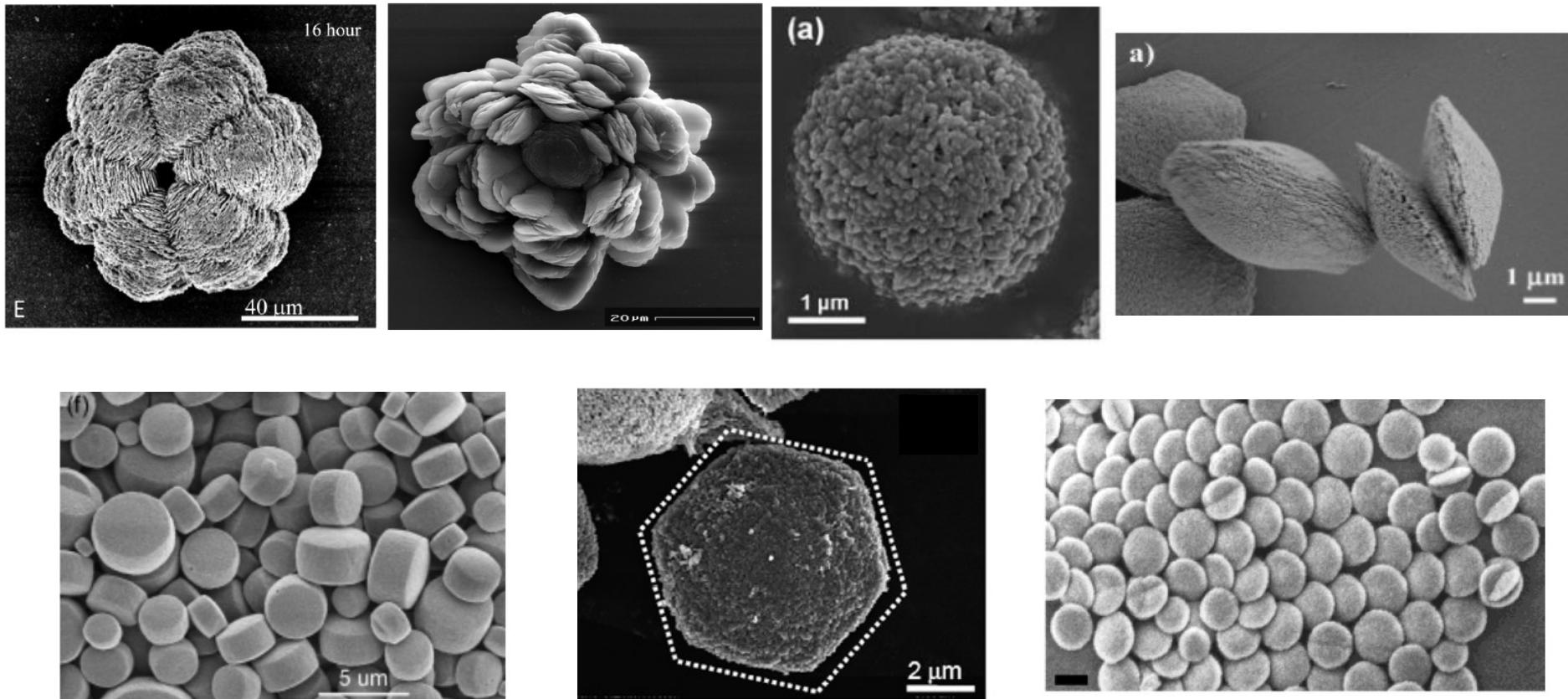
Saxifraga sempervivum, an alpine plant produces a greenish-white crust, which contains vaterite



Spicules from the simple sea creature Herdmania momus contain large single crystals of vaterite of higher quality than those in the synthetic vaterite used in previous structure determinations (ESRF)



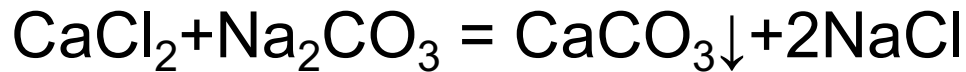
Variety of vaterite morphologies



- Trushina D.B. et al. Calcium carbonate vaterite particles for drug delivery: Advances and challenges // *Mater. Today Adv.* **2022**. Vol. 14, P. 100214
- Trushina D.B., Bukreeva T. V., Antipina M.N. Size-Controlled Synthesis of Vaterite Calcium Carbonate by the Mixing Method: Aiming for Nanosized Particles // *Cryst. Growth Des.* **2016**. Vol. 16, № 3. P. 1311–1319
- Mikheev A. V et al. Hybrid Core–Shell Microparticles Based on Vaterite Polymorphs Assembled via Freezing-Induced Loading // *Cryst. Growth Des.* **2023**. Vol. 23, № 1. P. 96–103

Vaterite

Size-controlled crystallization



Concentration of reagents

Temperature

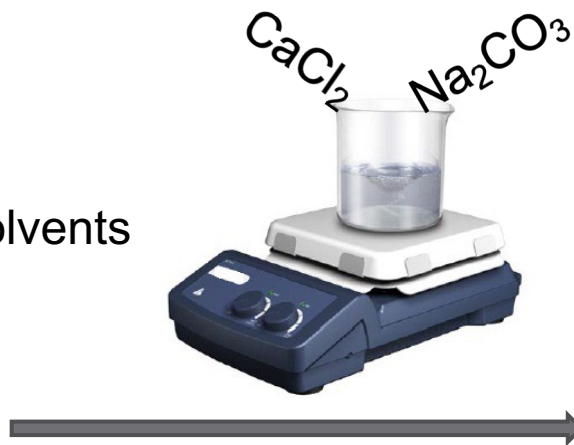
pH

Presence of additives, co-solvents

Volume ratio of reagents

Mixing time and intensity

Influence of external fields



Polymorph composition
Size
Form
Porosity

The main objective

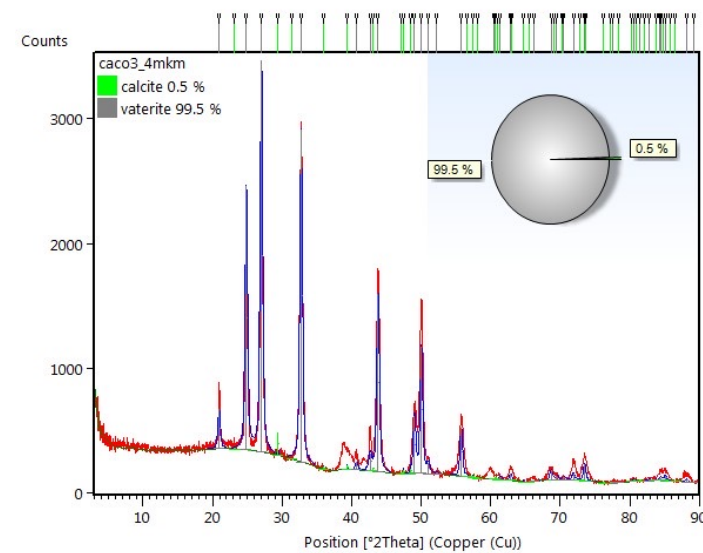
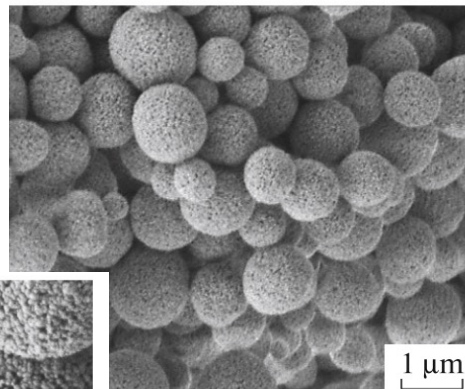
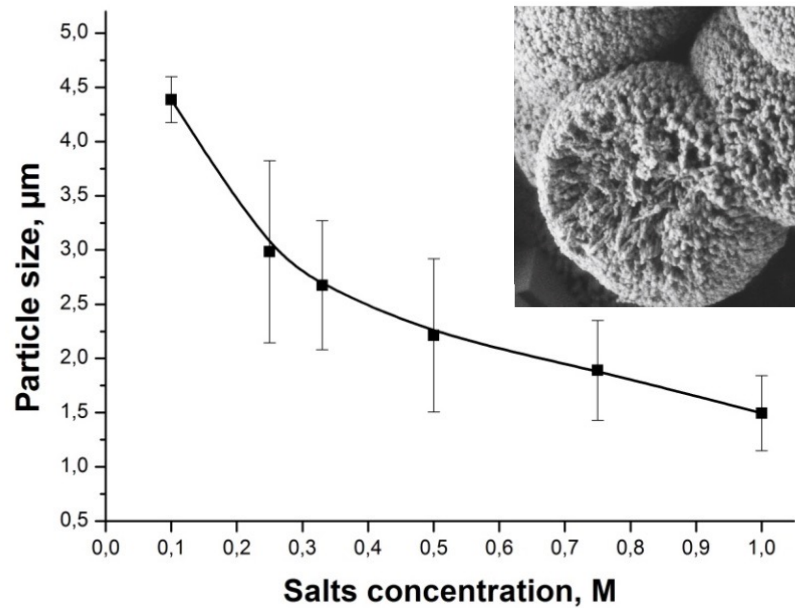
Crystallization of stable porous vaterite particles in a size-controlled manner

Focus on how to decrease the size

Micro-sized vaterite

Standard protocol allows vaterite with the size ranging from 4.5 μm to 1.5 μm

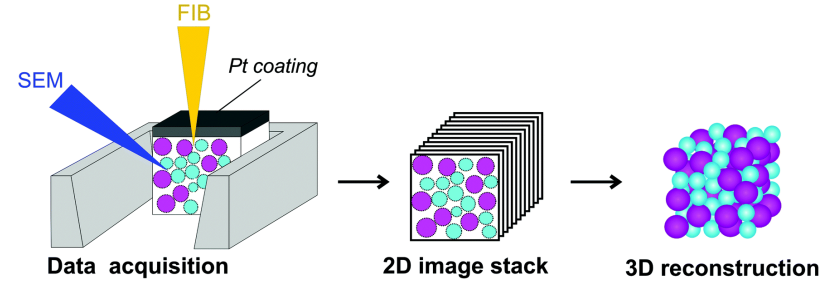
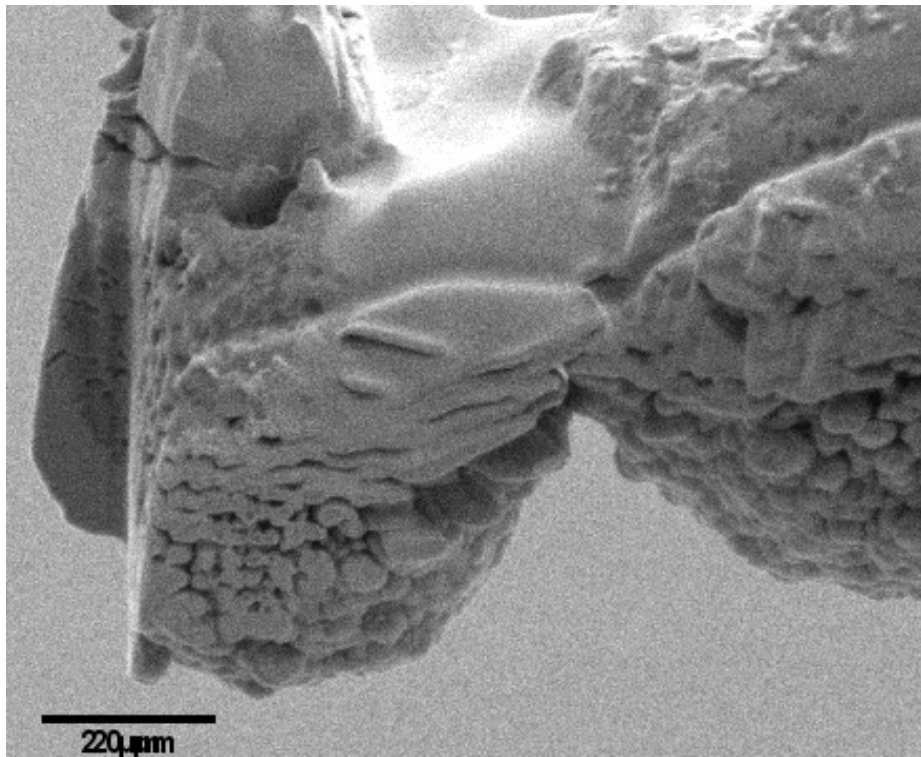
Influence of the concentration of reagents on the size



- Trushina, D. B.; Bukreeva, T. V.; Antipina, M. N. Size-Controlled Synthesis of Vaterite Calcium Carbonate by the Mixing Method: Aiming for Nanosized Particles. *Cryst. Growth Des.* **2016**, *16* (3), 1311–1319.

Micro-sized vaterite

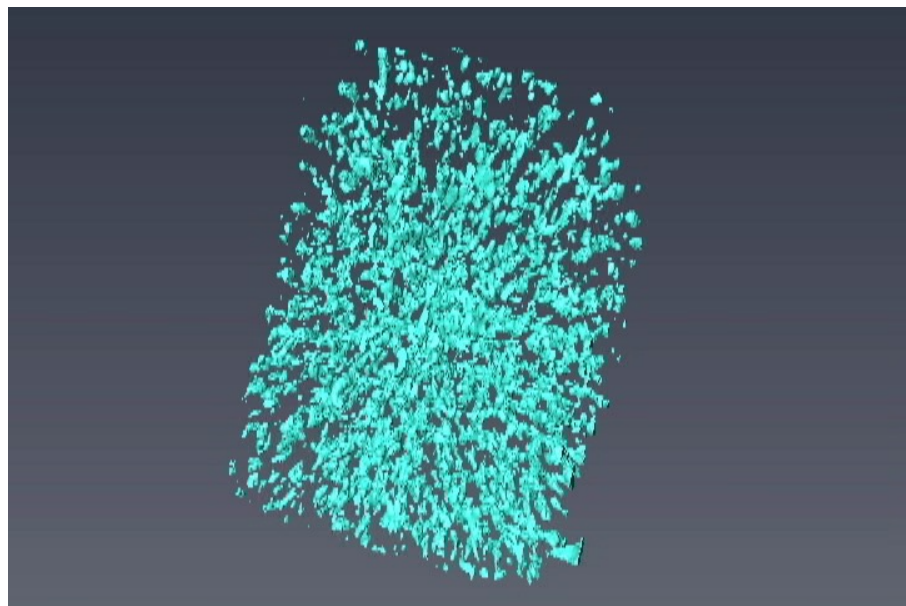
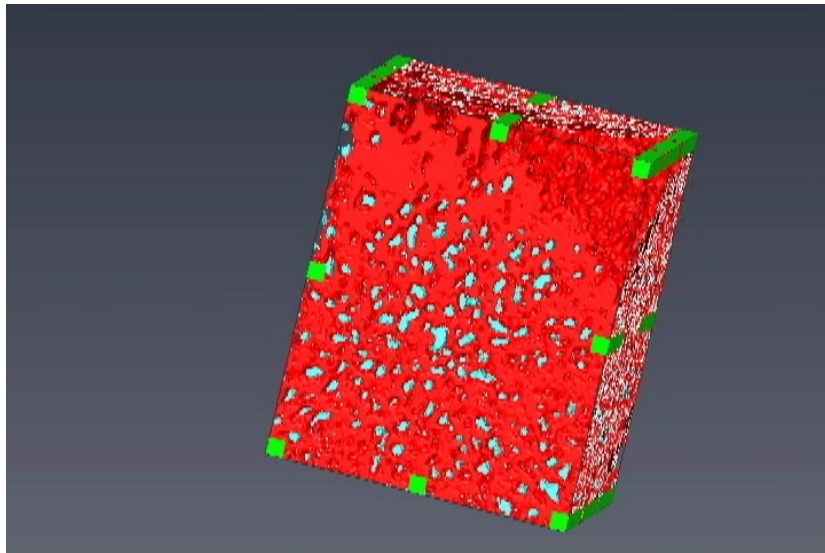
FIB (Ga ions) milling of a Pt-coated CaCO_3 particle



Micro-sized vaterite

3D reconstruction of vaterite particle structure according to SEM images

CaCO₃
Pores

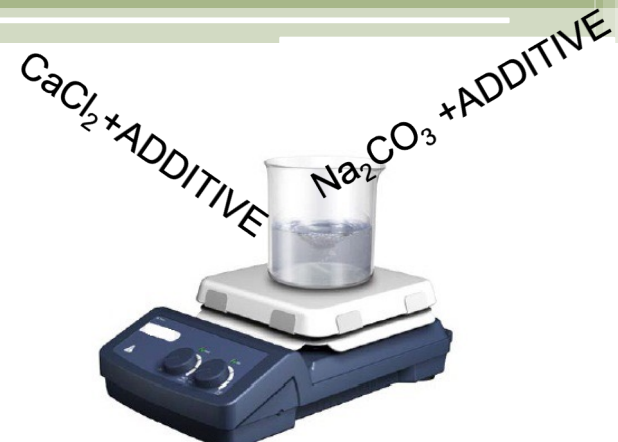
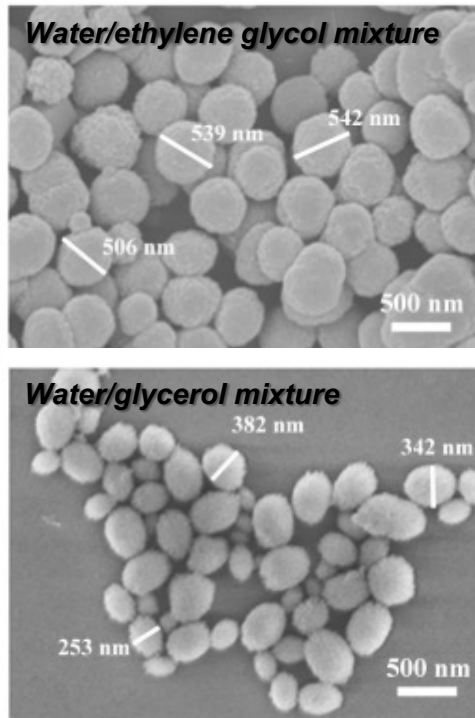
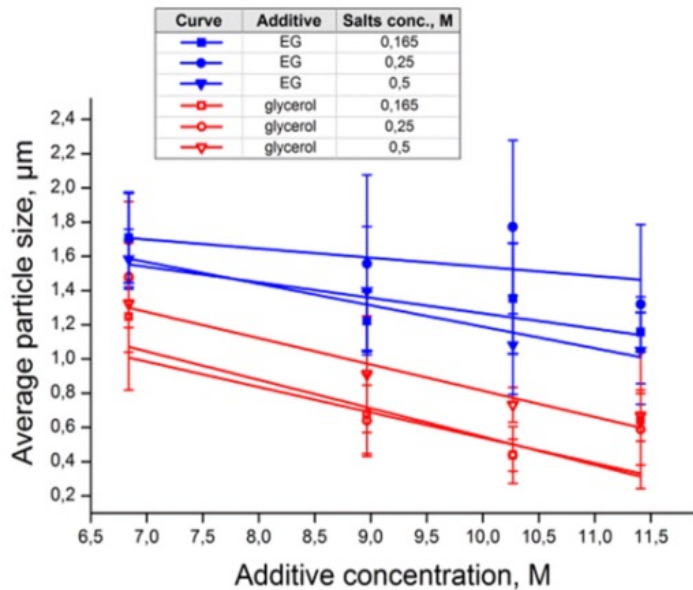


Submicron-sized vaterite

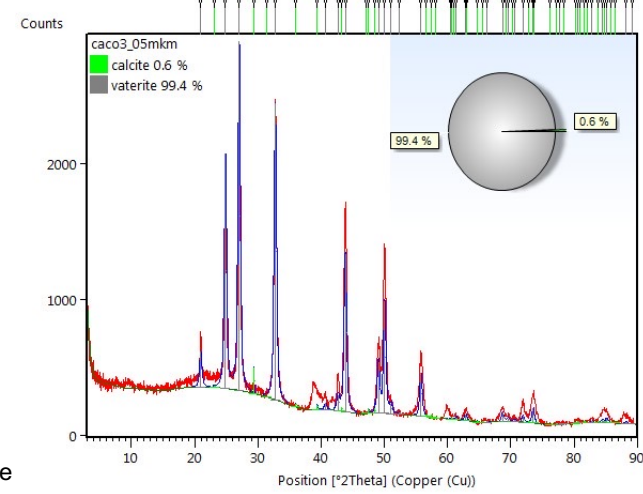
Modified protocol allows vaterite with the size ranging from $0.3\text{ }\mu\text{m}$ to $1.7\text{ }\mu\text{m}$

Optimization of the reaction parameters:

- ✓ Varying salts:co-solvent volume ratio (1:1 – 1:5)
- ✓ Different T (25°C – 40°C)
- ✓ Mixing time from 30s to 3h

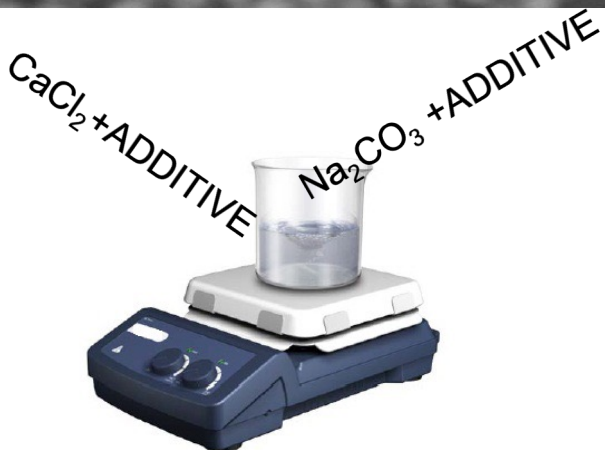
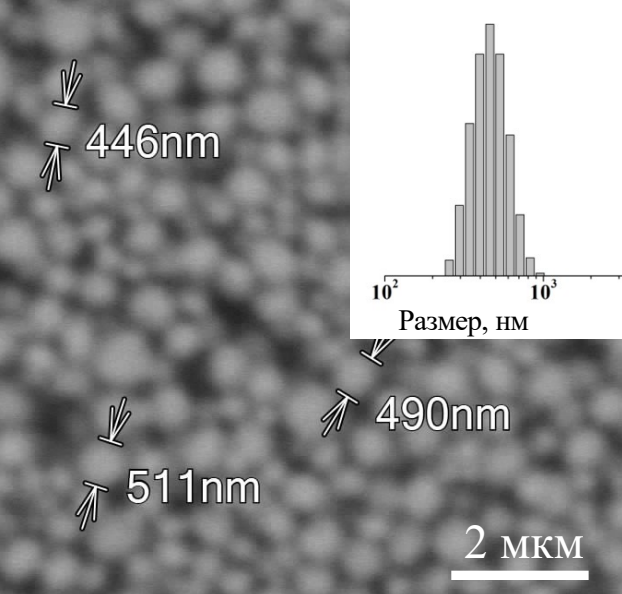


ADDITIVE (co-solvent): ethylene glycol/ glycerol



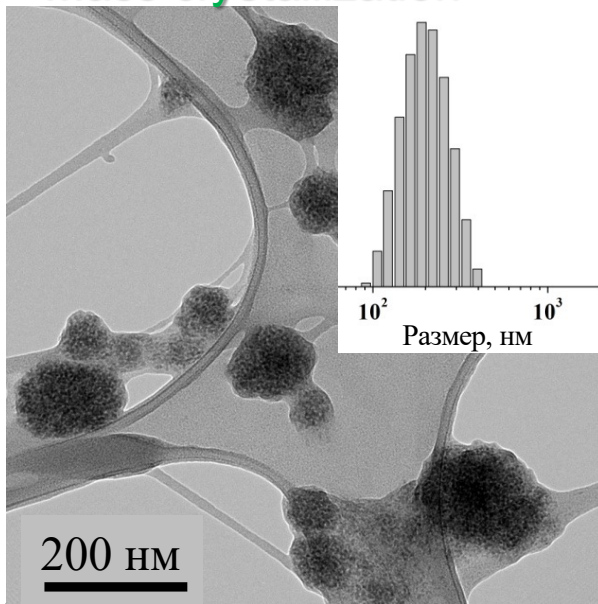
- Trushina, D. B.; Bukreeva, T. V.; Antipina, M. N. Size-Controlled Synthesis of Vaterite Calcium Carbonate by the Mixing Method: Aiming for Nanosized Particles. *Cryst. Growth Des.* **2016**, *16* (3), 1311–1319.
- Trushina, D. B.; Sulyanov, S. N.; Bukreeva, T. V.; Kovalchuk, M. V. Size Control and Structure Features of Spherical Calcium Carbonate Particles. *Crystallogr. Reports* **2015**, *60* (4), 570–577.

Mass crystallization



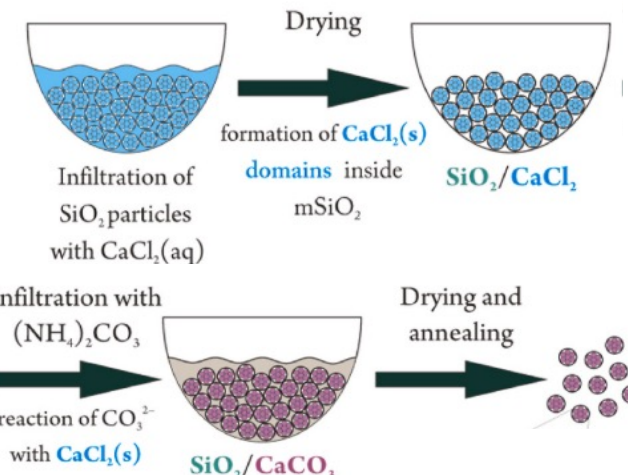
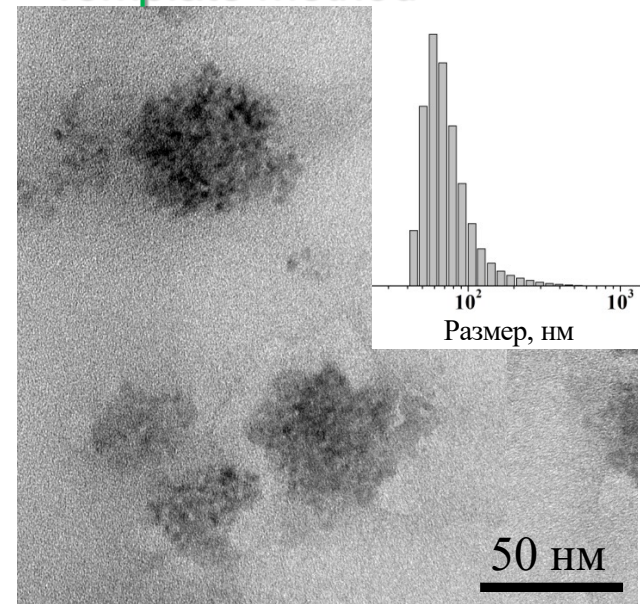
ADDITIVE (co-solvent):
ethylene glycol/glycerol

Mass crystallization



ADDITIVE: PEG+Tween-20+
DMEM + MgCl₂

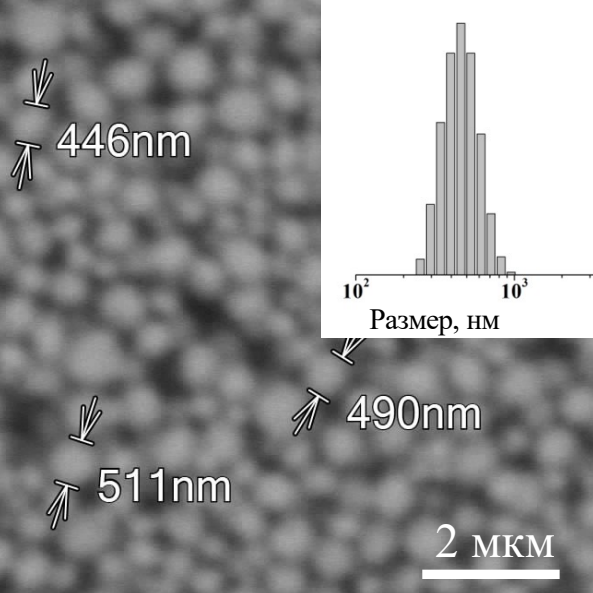
Template method



- D.A. Eurov et al. Microporous Mesoporous Mater. (2022)

- T. N. Pallaeva, A. V. Mikheev, D. N. Khmelenin, D. A. Eurov, D. A. Kurdyukov, V. K. Popova, E. V. Dmitrienko, D. B. Trushina. High-capacity calcium carbonate particles as pH-sensitive containers for doxorubicin, Crystallogr. Reports. 2 (2023) 309–315

Mass crystallization

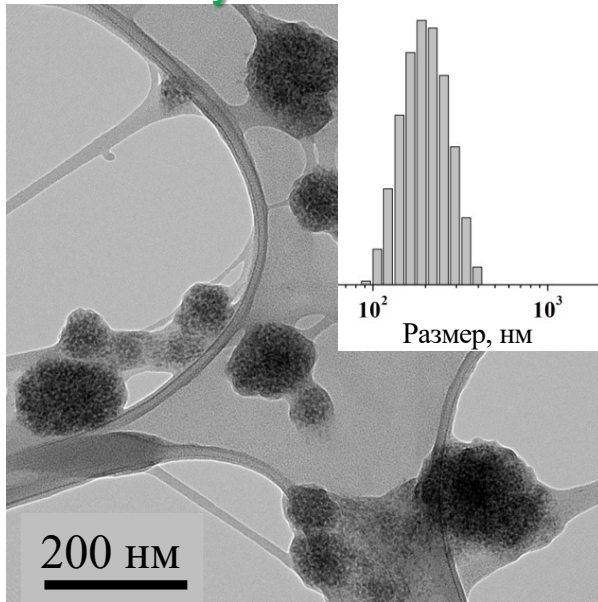


500±90 nm (CaCO₃– 500)

99.4% vaterite

6.5 wt%

Mass crystallization



172±75 nm (CaCO₃–200)

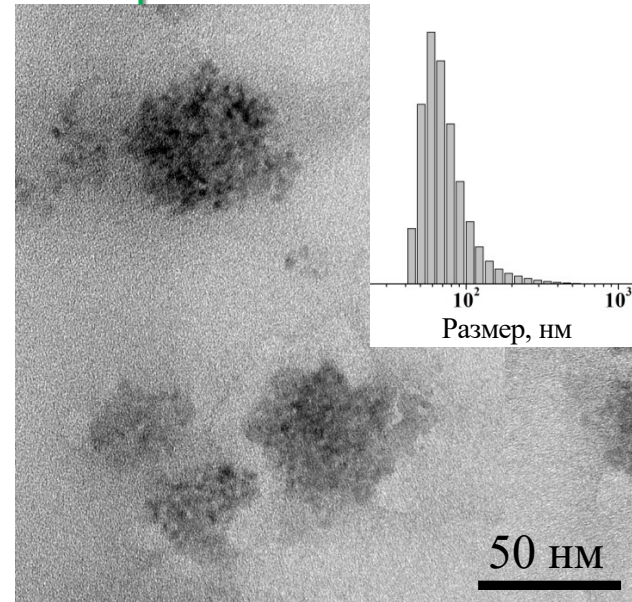
Polymorphic composition

Amorphous

Loading with doxorubicin

4.8 wt. %

Template method



65±15 nm (CaCO₃:Si:Fe–50)

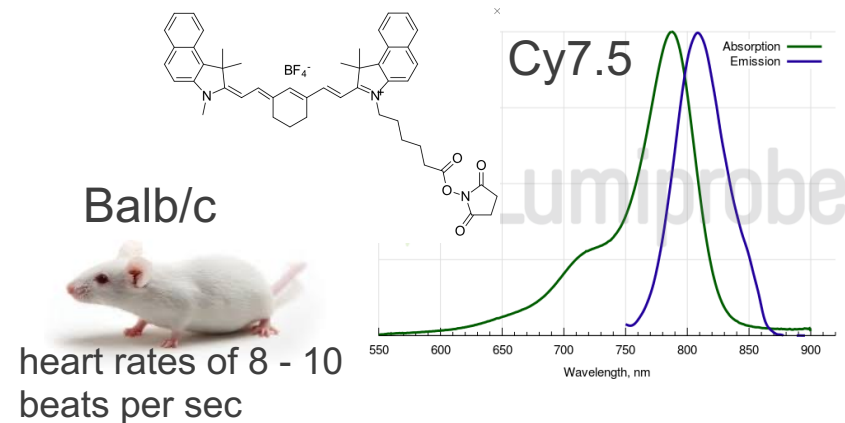
100% calcite

4.0 wt. %

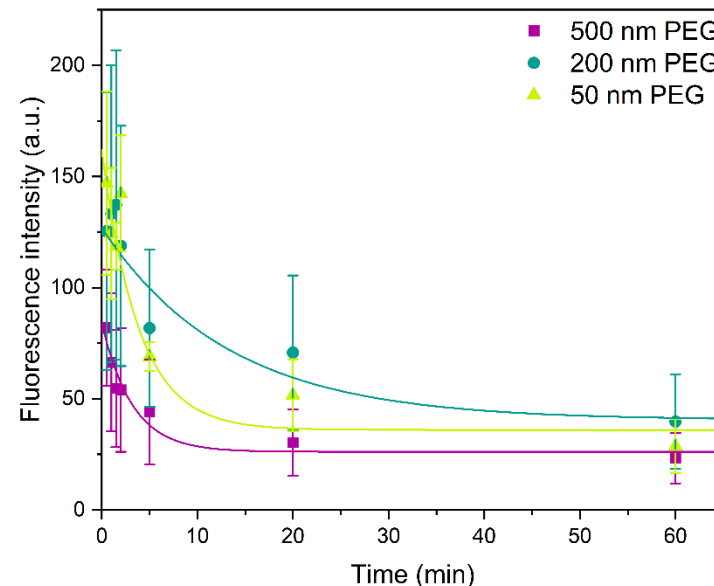
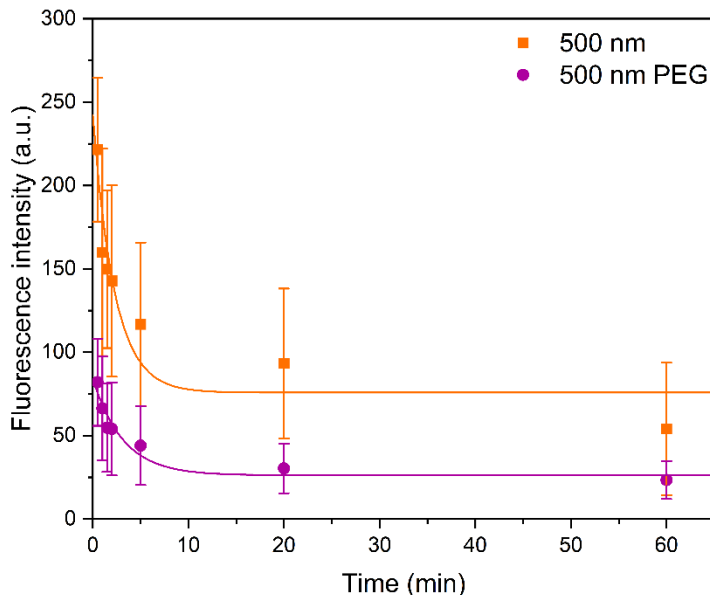
- T. N. Pallaeva, A. V. Mikheev, D. N. Khmelenin, D. A. Eurov, D. A. Kurdyukov, V. K. Popova, E. V. Dmitrienko, D. B. Trushina. High-capacity calcium carbonate particles as ph-sensitive containers for doxorubicin, Crystallogr. Reports. 2 (2023) 309–315

In vivo evaluation of 50/200/500nm CaCO₃ particles

Particle type	Blood half-life $t_{1/2}$, min
500 nm	1.6 ±0.7
500 nm/PEG	2.2±0.9
200 nm/PEG	9.2±4.7
50 nm/PEG	2.6±0.7

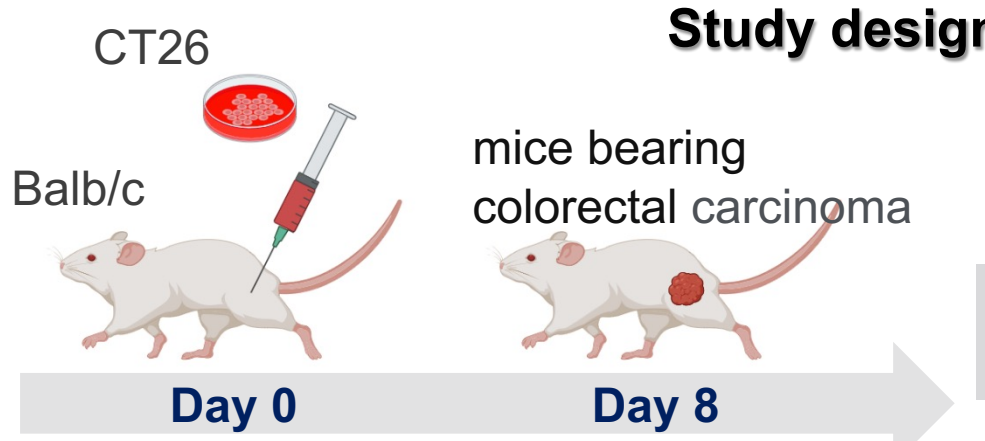


In vivo pharmacokinetic profiles of Cy7.5-labelled CaCO₃ in mice

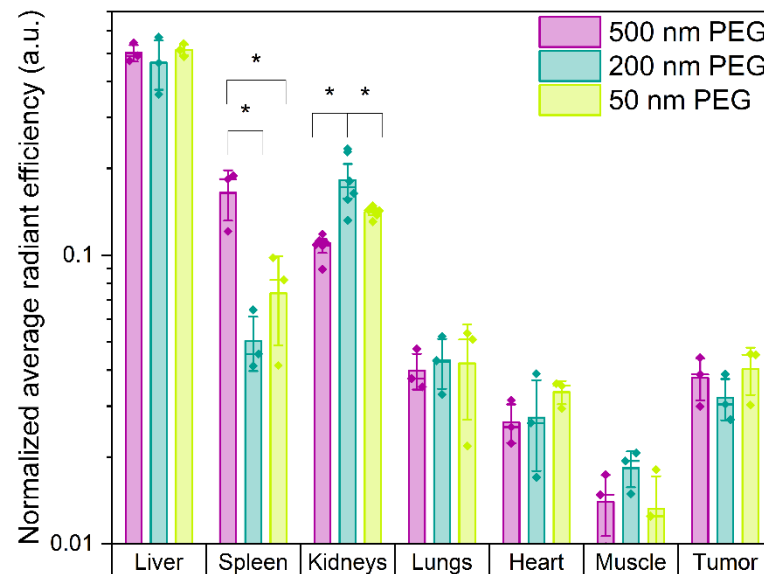


N=4

In vivo evaluation of 50/200/500nm CaCO₃ particles



In vivo biodistribution of Cy7.5-labelled CaCO₃ in mice (IVIS Spectrum CT)



N=4

* p = 0.05

Результаты и Выводы

Для синтеза CaCO_3 использовали методику массовой кристаллизации в растворах, а также темплатный синтез. Оптимизация условий кристаллизации позволила получить частицы CaCO_3 с размерами в диапазоне от 500 до 50 нм.

Для частиц 500нм циркуляция увеличивается при пэгилировании: $t_{1/2}$ увеличивается с 1.6 ± 0.7 до 2.2 ± 0.9 сек.

Для частиц 200нм $t_{1/2} = 9.2 \pm 4.7$ сек.

При внутривенном введении большинство субмикронных и наночастиц CaCO_3 — 500нм/PEG, CaCO_3 — 200нм/PEG и CaCO_3 —50/PEG аккумулируются в печени, селезенке, почках. Частицы одинаково накапливаются в опухоли в пределах погрешности. Т. о. применения наночастиц и полимерного покрытия недостаточно, чтобы значительно улучшить доставку препаратов к опухолевым клеткам.

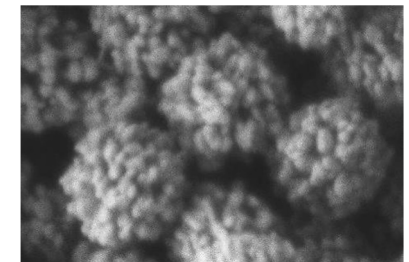
Acknowledgment

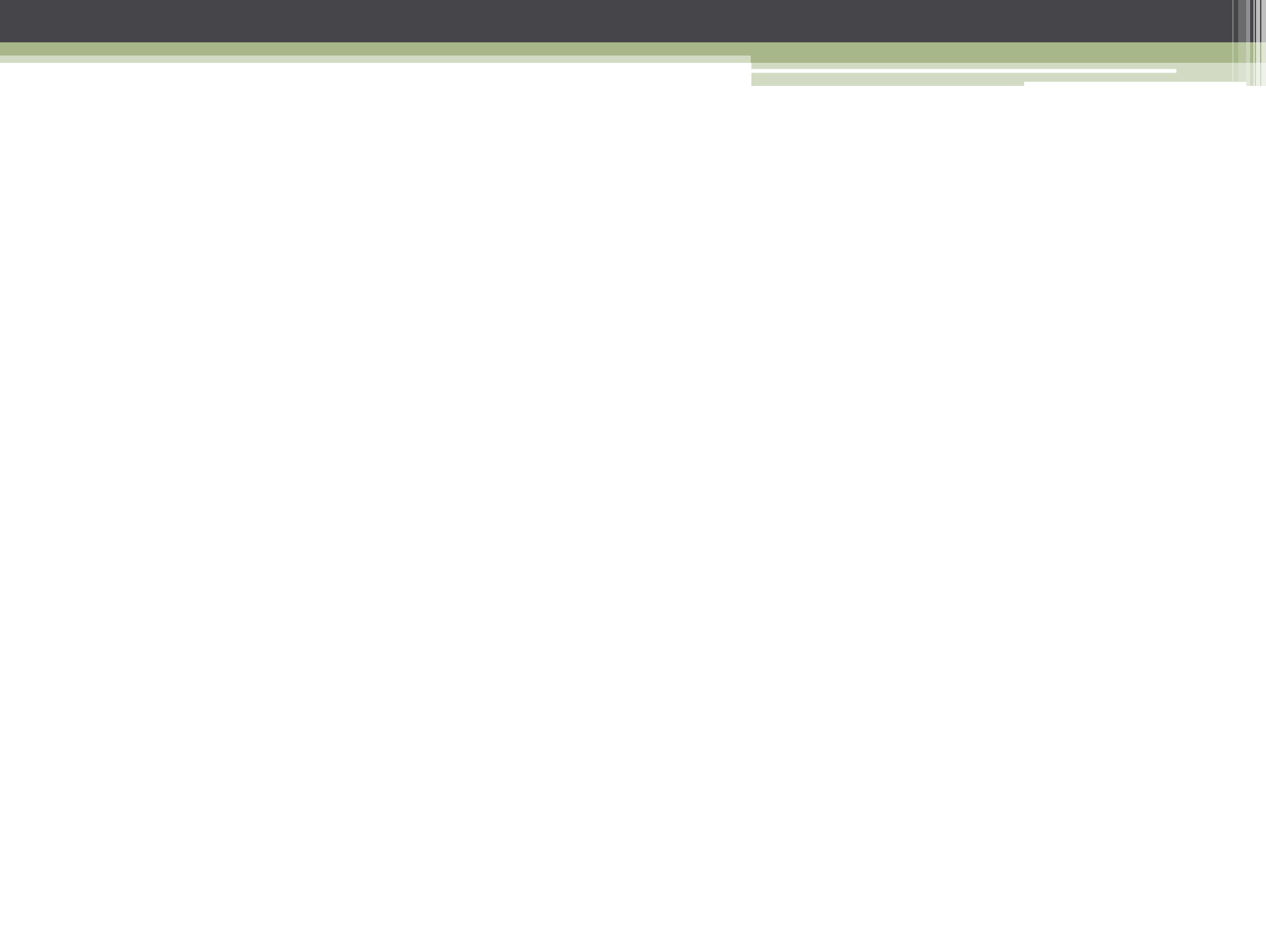


Работа поддержана грантом РНФ № 21-74-10058

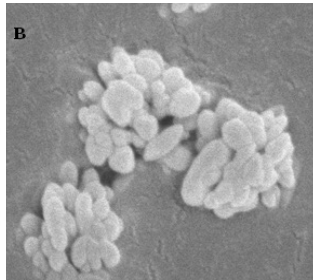
- ❖ ФНИЦ «Кристаллография и фотоника» РАН,
Сеченовский Университет, Москва
- ❖ ИБХ РАН, Москва
- ❖ ФТИ им. А.Ф. Иоффе, Санкт-Петербург
- ❖ Институт химической биологии и фундаментальной
медицины СО РАН, Новосибирск

Trushina.d@mail.ru





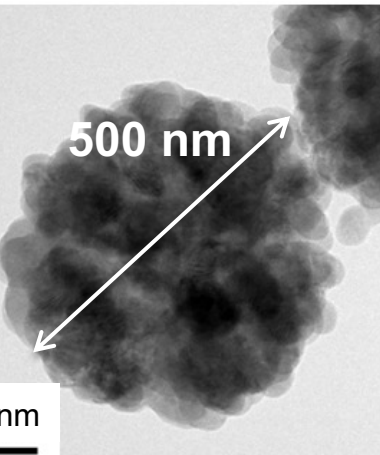
Two main types of vaterite architecture



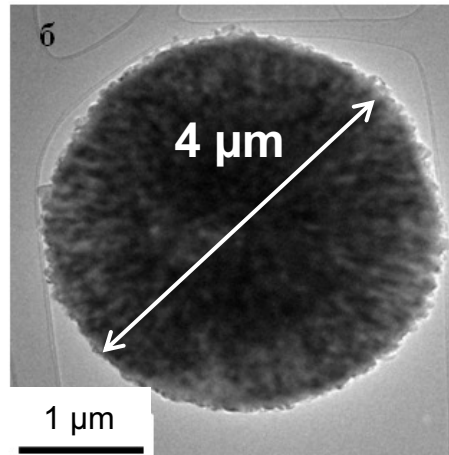
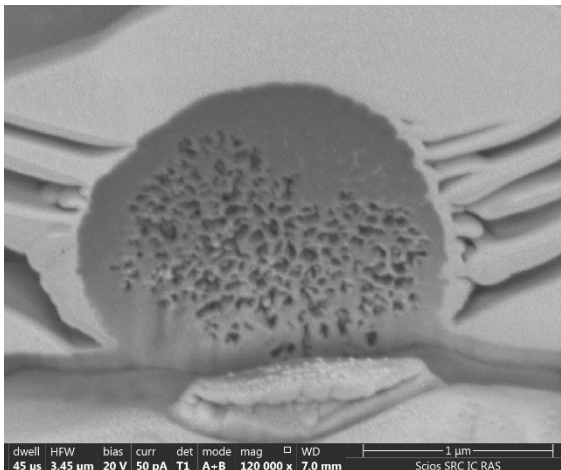
Framboids
(from fr. la framboise – raspberry)



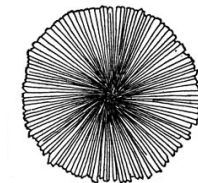
100 nm



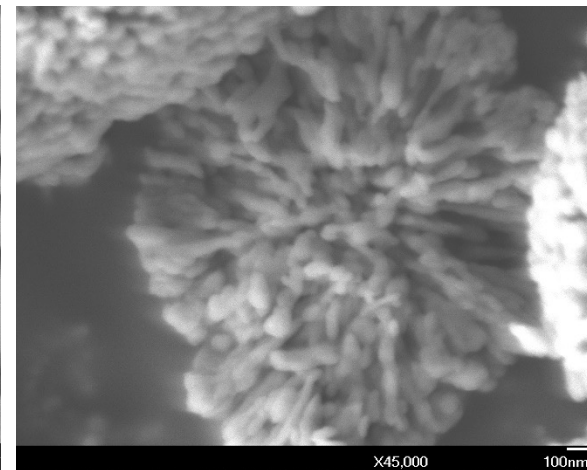
All directions are equal, frambooids are the result of crystal growth via oriented attachment of primary grains (non-classical crystal growth)



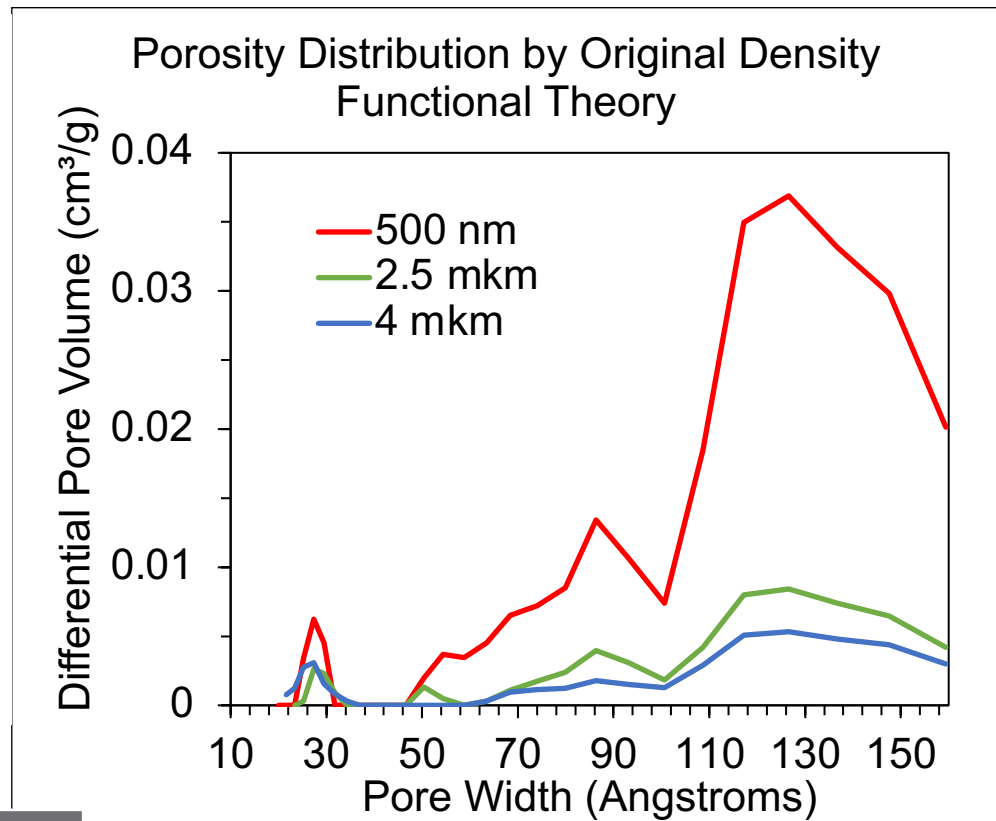
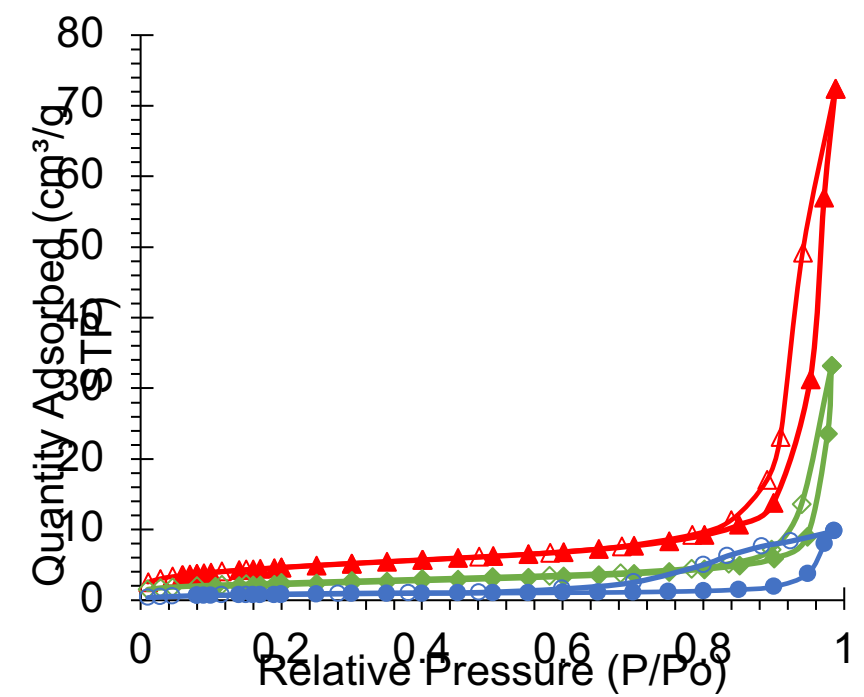
4 μm



Spherulites

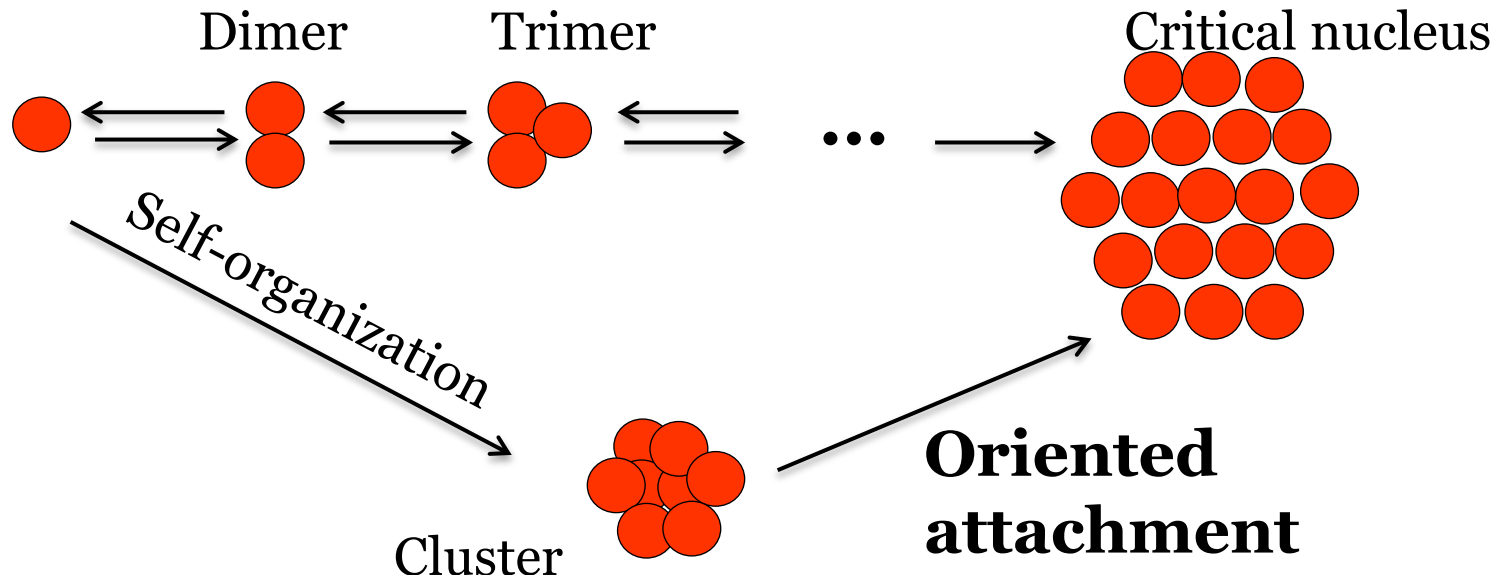


Spherulites are characterized by a radial-radiant internal structure due to the peculiarities of crystal growth

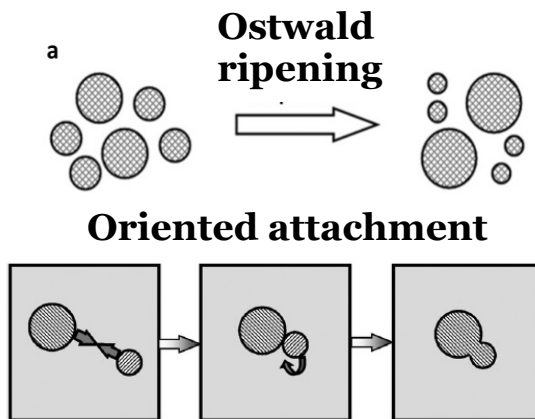


Diameter	BET Surface Area, m^2/g
500 nm	16.4
2.5 μm	7.8
4 μm	2.8

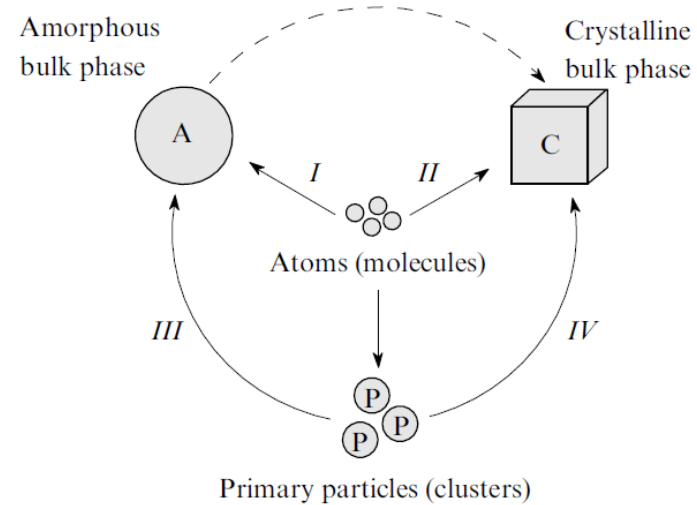
Classical theory (Ostwald ripening)

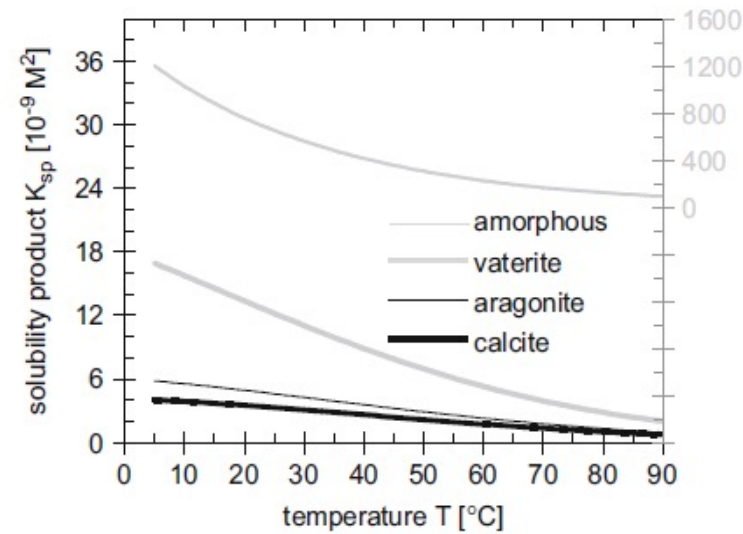
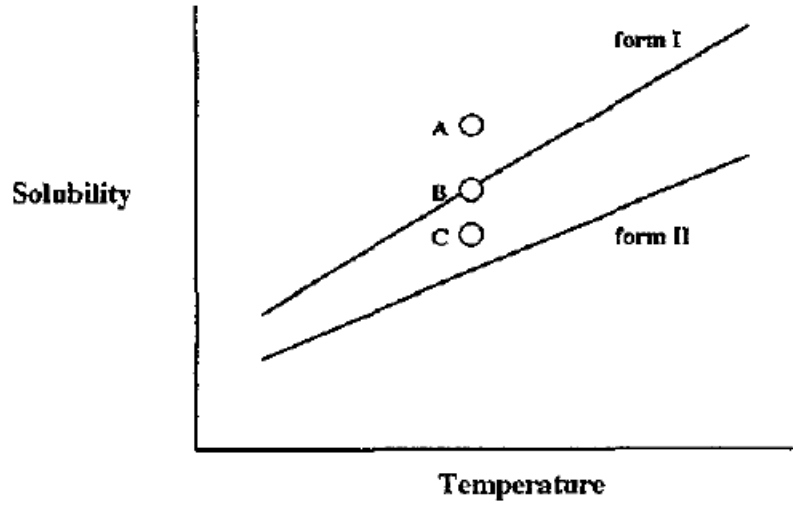


Building element: atom
VS nano cluster



Oriented attachment





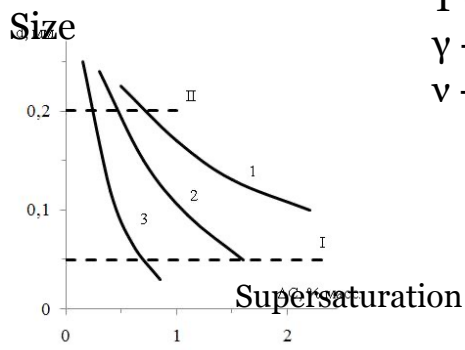
S. Khoshkhoo, J. Anwar, Crystallization of Polymorphs: the effect of solvent, *J. Phys. D: App. Phys.* 26 (1993) B90-B93

R. Beck, J.-P. Andreassen, The onset of spherulitic growth in crystallization of calcium carbonate, *J. Cryst. Growth* 312 (2010) 2226–2238.

Nuclei formation

Radius of spherical critical nucleus at given supersaturation

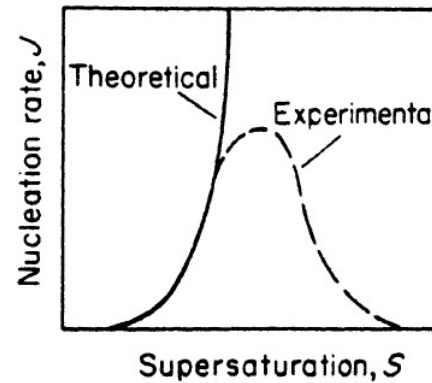
$$r_c = 2\gamma v / \mathbf{k} T \ln S$$



S – supersaturation,
 K – Boltzmann constant,
 T – temperature,
 γ - interfacial tension,
 v - molecular volume

Rate of nucleation – the number of nuclei formed per unit time per unit volume

$$J = A \exp \left[-\frac{16\pi\gamma^3 v^2}{3k^3 T^3 (\ln S)^2} \right]$$

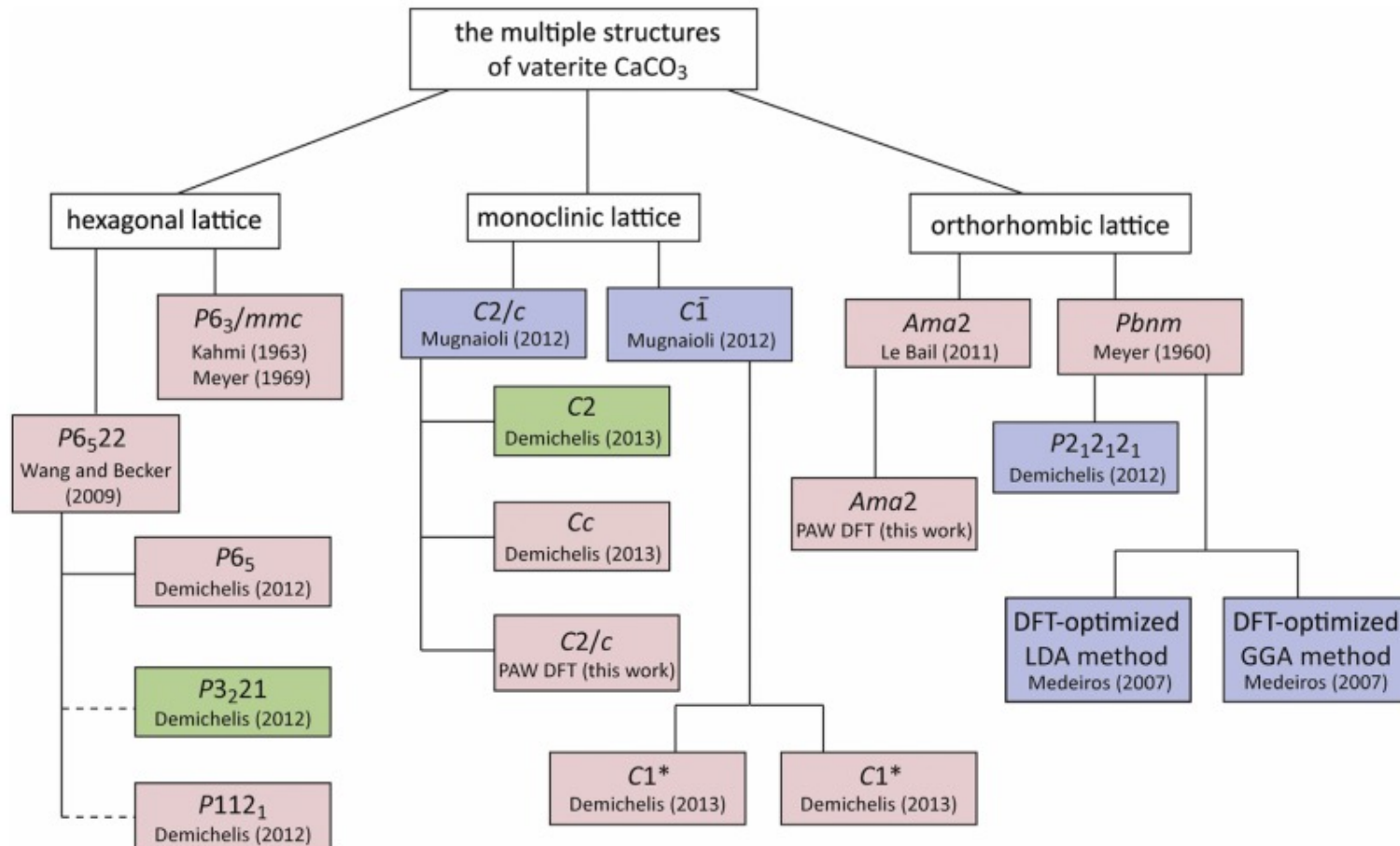


* Girshick, Steven L.; Chiu, Chia-Pin //The Journal of Chemical Physics, 1990, 93, 2, 1273

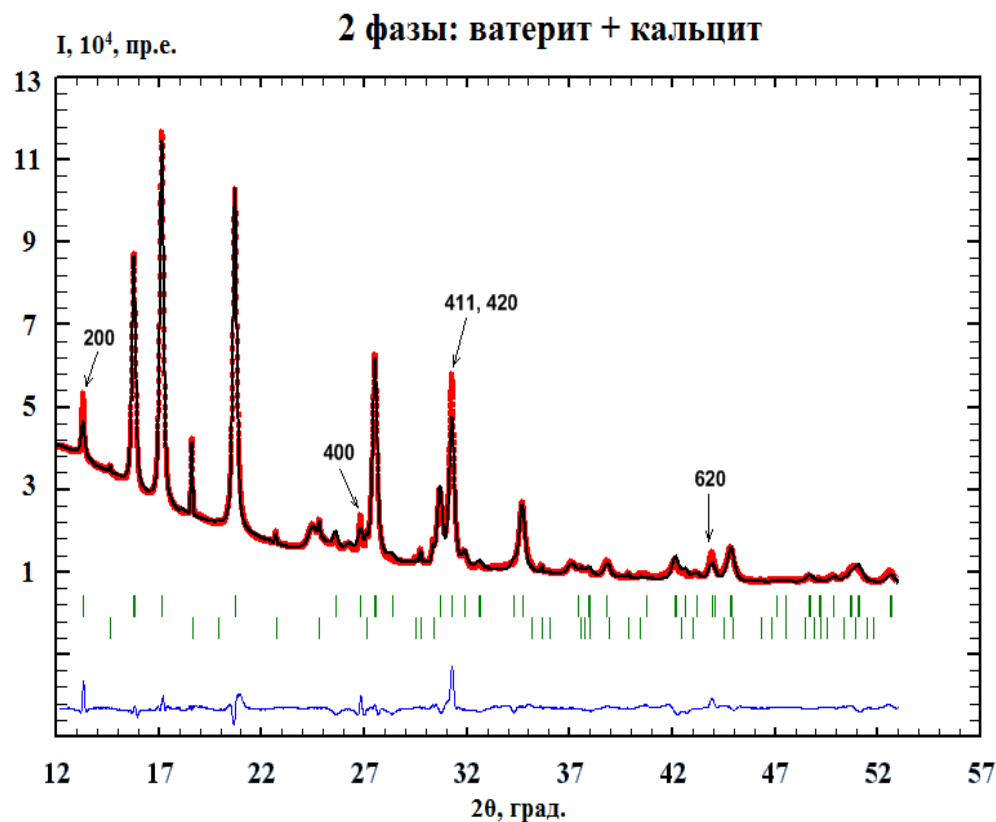
Разнообразие предложенных структур ватерита

K.M.N. Burgess, D.L. Bryce / Solid State Nuclear Magnetic Resonance ■ (■■■■) ■■■-■■■

Accepted 29 August 2014

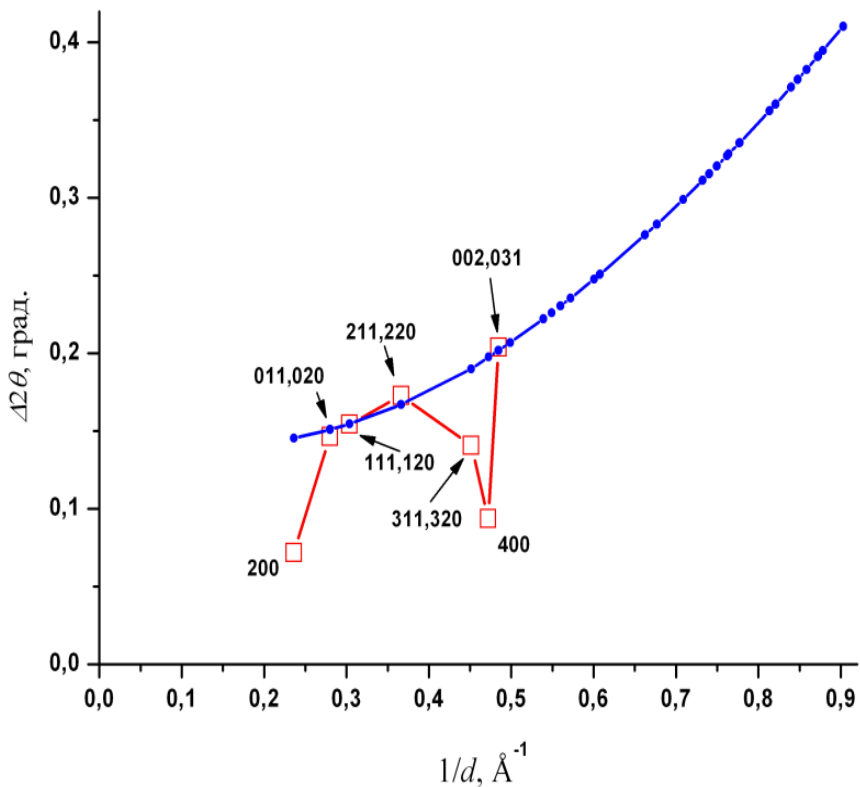


Vaterite Crystals Contain Two Interspersed Crystal Structures
Lee Kabalah-Amitai et al.
Science 340, 454 (2013);
DOI: 10.1126/science.1232139



Чем больше первый индекс h рефлекса, тем уже пик, т.е. тем больше размер наночастиц в направлении параметра решётки a .

Исходная рентгенограмма и результат уточнения методом Ритфельда для одного из образцов карбоната кальция



Зависимость ПШПВ дифракционных максимумов от обратного межплоскостного расстояния (построение по Williamson-Hall)

Каждый символ на гладкой линии (рассчитанной методом Ритфельда) означает ФУ (ПШПВ) для конкретного пика в модели Le Bail. Величины, обозначенные полыми квадратами, получены отдельно интерполяцией функцией pseudo-Voigt на линейном фоне.

Используя методику Вильямсона-Холла и соотношение Шеррера получены размеры нанокристаллитов (области когерентного рассеяния)-значения длин главных осей эллипсоида $2r_a = 1000(90) \text{ \AA}$ и $2r_b \approx 2r_c = 500(50) \text{ \AA}$.

A new structural model for disorder in vaterite from first-principles calculations[†]

Raffaella Demichelis,^{*a} Paolo Raiteri,^a Julian D. Gale^a and Roberto Dovesi^b

Received 31st July 2011, Accepted 13th October 2011

DOI: 10.1039/c1ce05976a

Table 1 Structures proposed for vaterite: space group (*SG*) and lattice parameters [Å]

Reference	<i>SG</i>	<i>a</i>	<i>b</i>	<i>c</i>
Meyer ¹¹	<i>Pbnm</i>	4.13	7.15	8.48
McConnell ¹²	<i>P6₃22</i>	7.135	7.135	8.524
Kahmi, ¹³ Sato and Matsuda ¹⁴	<i>P6₃/mmc</i>	4.13	4.13	8.49
Bradley <i>et al.</i> ¹⁵	<i>P6₃22</i>	7.135	7.135	8.524
Meyer, ⁷ Gabrielli <i>et al.</i> ⁶	<i>P6₃/mmc^a</i>	7.15	7.15	16.96
Dupont <i>et al.</i> ¹⁶	<i>P6₃/mmc^a</i>	7.169	7.169	16.98
Le Bail <i>et al.</i> ⁹	<i>Amd2</i>	8.7422	7.1576	4.1265
Medeiros <i>et al.</i> ¹⁷	<i>Pbnm^b</i>	4.531	6.640	8.480
Wang and Becker ¹⁸	<i>P6₅22^b</i>	7.290	7.290	25.302

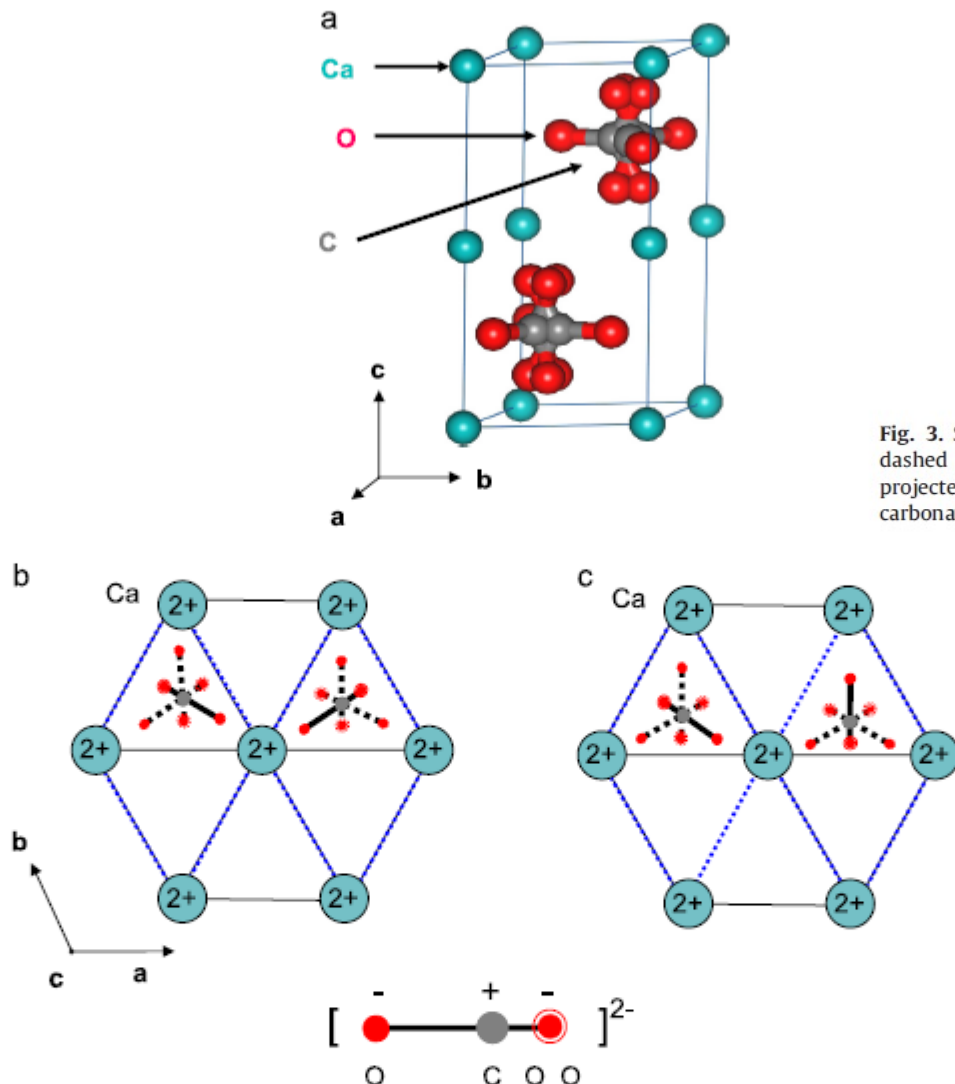


Fig. 2. (a) Crystal structure of vaterite with disordered CO_3^{2-} group [16]. Each CO_3^{2-} has a one-third occupancy. Ca^{2+} ions form a hexagonal lattice. (b) and (c) Schematic view of Ca^{2+} lattice (shown as $2+$ charge inside a circle) and CO_3^{2-} orientations. Thin dashed lines highlight the pseudo unit cells. Three possible orientations of CO_3^{2-} ions are shown in dashed and solid symbols. The configuration in (b) where the two neighboring CO_3^{2-} ions are pointing to the same edge of the prisms is less stable than the one in (c) where the two neighboring CO_3^{2-} ions are pointing to different edges because of electrostatic repulsion between the oxygen atoms of CO_3^{2-} in the former configuration.

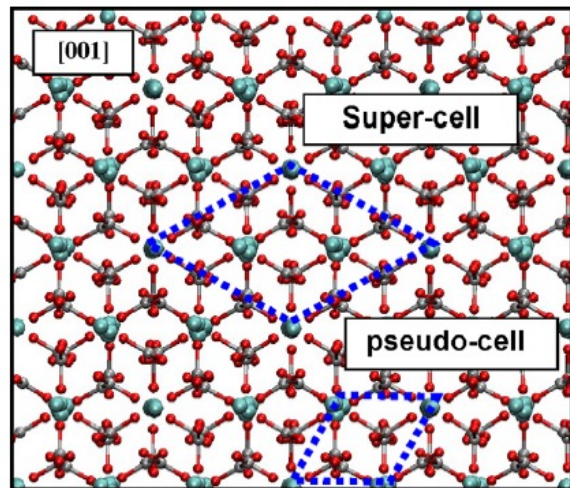


Fig. 3. Structure of a snapshot from molecular dynamics simulation with the dashed lines highlighting the basic pseudocell and supercell. The structure is projected on (001) plane. The large balls are calcium atoms. The balls and sticks are carbonate groups.

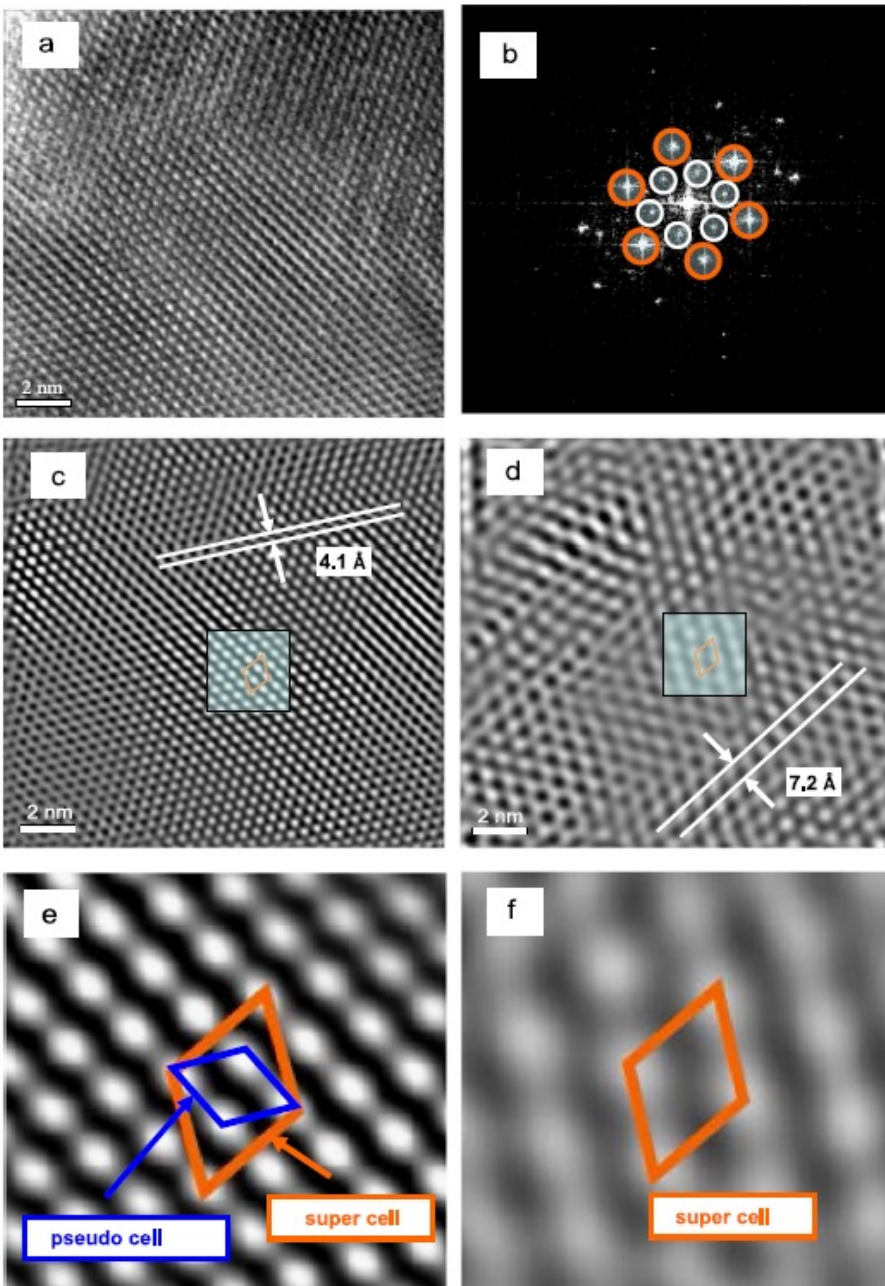
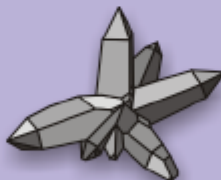


Fig. 6. (a) An HRTEM image shows the threefold symmetry along [001]. (b) A fast Fourier transform corresponding to the image (a). Two sets of diffraction peaks present and were highlighted with small and larger circles, respectively. (c) The HRTEM image generated from the primary diffraction peaks in Fig. 4b. (d) The HRTEM image generated from the satellite diffraction peaks in Fig. 4b. (e) The HRTEM image of the highlighted region in Fig. 4c. (f) The HRTEM image of the highlighted region in Fig. 4d. The basic lattice and superlattice are highlighted in Figs. 4e, f.

precursors to polymorphs?

| hydrous |

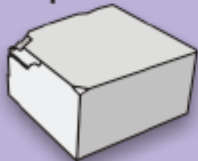


Ikaite
monoclinic



Monohydrocalcite
trigonal

| anhydrous |



Calcite
trigonal



Aragonite
orthorhombic



Vaterite
hexagonal (?)